THE JOURNAL OF BIOLOGICAL CHEMISTRY VOL. 284, NO. 29, pp. 19694–19704, July 17, 2009

Interdependence of Laminin-mediated Clustering of Lipid Rafts and the Dystrophin Complex in Astrocytes*[S]

Received for publication, December 9, 2008, and in revised form, April 17, 2009 Published, JBC Papers in Press, May 18, 2009, DOI 10.1074/jbc.M109.010090

Geoffroy Noël, Daniel Kai Long Tham, and Hakima Moukhles[1]

From the Department of Cellular and Physiological Sciences, University of British Columbia, Vancouver V6T 1Z3, Canada

Astrocyte endfeet surrounding blood vessels are active domains involved in water and potassium ion transport crucial to the maintenance of water and potassium ion homeostasis in brain. A growing body of evidence points to a role for dystroglycan and its interaction with perivascular laminin in the targeting of the dystrophin complex and the water-permeable channel, aquaporin 4 (AQP4), at astrocyte endfeet. However, the mechanisms underlying such compartmentalization remain poorly understood. In the present study we found that AQP4 resided in Triton X-100-insoluble fraction, whereas dystroglycan was recovered in the soluble fraction in astrocytes. Cholesterol depletion resulted in the translocation of a pool of AQP4 to the soluble fraction indicating that its distribution is indeed associated with cholesterol-rich membrane domains. Upon laminin treatment AQP4 and the dystrophin complex, including dystroglycan, reorganized into laminin-associated clusters enriched for the lipid raft markers GM1 and flotillin-1 but not caveolin-1. Reduced diffusion rates of GM1 in the laminin-induced clusters were indicative of the reorganization of raft components in these domains. In addition, both cholesterol depletion and dystroglycan silencing reduced the number and area of laminin-induced clusters of GM1, AQP4, and dystroglycan. These findings demonstrate the interdependence between laminin binding to dystroglycan and GM1-containing lipid raft reorganization and provide novel insight into the dystrophin complex regulation of AQP4 polarization in astrocytes.

The basement membrane is a specialized extracellular matrix (ECM)[2] composed of collagen, fibronectin, perlecan, agrin, and laminin. Several studies have focused on the involvement of these ECM molecules in the formation and maturation of neuromuscular junctions (1–4) and interneuronal synapses (5). More recently, much effort has been made by our group and others to understand the role of these molecules at the interface of astroglia and blood vessels (6–8). Laminin is highly expressed at the perivascular ECM, and the laminin receptor, dystroglycan (α-DG), together with many other components of the dystrophin-associated protein (DAP) complex, is particularly enriched at astrocyte endfeet abutting the blood vessels (9–11). The binding of laminin to α-DG at these specialized astrocyte domains in brain plays a key role in the polarized distribution of components of the DAP complex (6, 12).

Multiple lines of evidence indicate that the DAP complex is crucial for the functional distribution both of the water-permeable channel, AQP4, and the inwardly rectifying potassium channel, Kir4.1, at astrocyte endfeet. Indeed, mutations in the dystrophin gene, deletion of α-syntrophin, or loss of laminin binding to α-DG caused by a mutation in the Large1 glycosyltransferase result in a dramatic reduction of the expression of AQP4 and Kir4.1 at perivascular astrocyte endfeet (6, 7, 12–15). The mislocalization of AQP4 in the dystrophin mutant and α-syntrophin null mice results in delayed onset of brain edema and K^+ clearance (16–18). Collectively, these studies highlight a cooperative role of the ECM and both the extracellular and cytoplasmic components of the DAP complex in the proper targeting of proteins to functional domains of astrocytes leading to the regulation of electrolyte balance and fluid movement.

Although the role of DG in targeting other members of the DAP complex (6) as well as AQP4 and Kir4.1 to astrocyte endfeet has been well established (12), the mechanisms underlying this highly organized distribution remain poorly understood. In C2C12 myotubes, agrin triggers AChR clustering, a DG-dependent process, through the coalescence of lipid rafts, which is necessary for proper AChR gating functions (19–21). In oligodendrocytes, laminin induces the relocalization of α6β1 integrin to lipid rafts containing PDGFαR, thereby providing a potential mechanism for the incorporation of cell survival signals (22). Lipid rafts are defined as small (10–200 nm), heterogeneous, highly dynamic, sterol- and sphingolipid-enriched domains that compartmentalize cellular processes. These small rafts can sometimes be stabilized to form larger platforms through protein-protein and protein-lipid interactions (23). Indeed, the immunological synapse is a good example where rafts are brought together to form large functional membrane domains (24). At the immunological synapse, agrin induces the clustering of lipid rafts and their colocalization with CD3 and CD28 complex surface antigens as well as with Lck tyrosine kinase leading to T cell activation (24). Together, these studies

* This work was supported by grants from the Canadian Institutes of Health Research, Muscular Dystrophy Canada, and Amyotrophic Lateral Sclerosis Society of Canada (to H. M.) and by a University Graduate Fellowship (to G. N.).

[S] The on-line version of this article (available at http://www.jbc.org) contains supplemental Figs. S1–S8.

[1] To whom correspondence should be addressed: Dept. of Cellular and Physiological Sciences, University of British Columbia, Life Sciences Centre, 2350 Health Sciences Mall, Vancouver V6T 1Z3, Canada. Tel.: 604-822-7882; Fax: 604-822-2316; E-mail: moukhles@interchange.ubc.ca.

[2] The abbreviations used are: ECM, extracellular matrix; DG, dystroglycan; AQP4, aquaporin 4 channel; GM1, monosialotetrahexosylganglioside; GD1, IV NeuAc,III 6 NeuAcGg Ose_4-ceramide; DRM, detergent-resistant membrane; PBS, phosphate-buffered saline; DAP, dystrophin-associated protein; AChR, acetylcholine receptor; CtxB, cholera toxin subunit B; TfR, transferrin receptor; E, embryonic day; siRNA, small interference RNA; FITC, fluorescein isothiocyanate; siCTL, control scrambled siRNA; MAPK, mitogen-activated protein kinase.

provide evidence for a functional role of ligand-induced clustering of lipid rafts.

We have previously shown that laminin induces the coclustering of the DAP complex with Kir4.1 and AQP4 in glial cell cultures (8, 25). Moreover, *in vivo* studies have shown that the perivascular localization of these channels and several components of the DAP complex at astrocyte endfeet require the interaction of laminin with α-DG (6, 12). In light of these data we asked whether lipid rafts contribute to the laminin-DG-dependent compartmentalization of the DAP complex and AQP4 to key active domains of astrocytes. We show here using fluorescently labeled cholera toxin subunit B (CtxB), a common marker for GM1-containing lipid rafts, that laminin induces a dramatic reorganization of GM1 into large clusters or macrodomains that colocalize extensively with components of the DAP complex in cortical astrocyte cultures. Laminin-mediated clustering of AQP4 is dependent both on cholesterol-sensitive lipid rafts and the DAP complex bringing novel insight into ECM-dependent membrane domain organization and the mechanisms underlying the polarized distribution of these proteins in astrocytes.

MATERIALS AND METHODS

Antibodies—The following antibodies were used in the present study: rabbit anti-AQP4 against rat glutathione *S*-transferase AQP4 corresponding to residues 249–323 (Alomone Laboratories, Jerusalem, Israel), rabbit anti-laminin against purified mouse Engelbreth-Holm-Swarm sarcoma laminin, which recognizes laminin α1, β1, and γ1 chains, rabbit polyclonal antibody to dystrophin (a generous gift from Dr. S. Carbonetto, McGill University, Montreal, Quebec, Canada), rabbit anti-caveolin-1 against the N terminus of human caveolin-1 (Santa Cruz Biotechnology, Santa Cruz, CA), rabbit anti-GFAP against the glial fibrillary acidic protein isolated from cow spinal cord (Dako, Mississauga, Ontario, Canada), mouse anti-β-DG, 43DAG1/8D5, against the 15 of the last 16 amino acids at the C terminus of the human dystroglycan sequence (Novocastra Laboratories, Newcastle-upon-Tyne, UK), mouse anti- syntrophin, SYN1351, against *Torpedo* syntrophin (Affinity Bioreagents), mouse anti-flotillin-1 (BD Biosciences), mouse anti-α-tubulin against residues 426–450 (Abcam), mouse anti-TfR against the transferrin receptor (TfR) against residues 3–28 of the human TfR tail (Zymed Laboratories Inc.), and mouse anti-utrophin (8A4, Developmental Studies Hybridoma Bank, University of Iowa).

Astrocyte Primary Cultures—Primary cortical astrocyte cultures were prepared from embryonic day 18 rats (E18) (Sprague-Dawley, Charles River). Cortices were dissected, and meninges and choroid plexus were removed. They were then cut into small pieces and incubated for 25 min with trypsin (3.0 mg/ml, Invitrogen). Dissociated cortices were then plated in culture flasks and grown in Dulbecco's modified Eagle's medium supplemented with 10% fetal bovine serum, 1% penicillin-streptomycin, and 1 mM L-glutamine (Invitrogen) for 2–3 weeks. The culture medium was changed every 3 days. To remove microglia and oligodendrocyte progenitors, the flasks were shaken the day following the plating. After trypsinization, the cells were plated on glass coverslips coated with poly-D-lysine (0.1 mg/ml, Sigma) in 24-well plates at a density of $200–250 \times 10^3$ cells/ml. Two days after plating, the cells were treated for 8 h with either 30 nM Engelbreth-Holm-Swarm sarcoma laminin-1 (Sigma-Aldrich), C-agrin 4,8 (10 nM), C-agrin 0,0 (10 nM, generous gift from Dr. M. Ferns, University of California, Davis), or with 100 nM fibronectin (Sigma).

siRNA Transfections and Cholesterol Depletion and Repletion—Astrocytes were transfected in suspension before plating with 100 nM *Dag1* and *Aqp4* siRNAs (siGENOME and ON-TARGETplus SMARTpool siRNA reagents, Dharmacon) and control siRNA (ON-TARGETplus siCONTROL nontargeting siRNA, Dharmacon) using Lipofectamine 2000 (Invitrogen), following the manufacturer's protocol. One day and a half after plating, astrocytes were treated for 8 h with 30 nM laminin-1 (Sigma-Aldrich) and subsequently analyzed by immunofluorescence. The efficiency of transfection was assessed by immunoblot analysis of proteins extracted on ice using an extraction buffer (25 mM Tris, pH 7.4, 25 mM glycine, and 150 mM NaCl) containing 1% Triton X-100, 1× Complete protease inhibitor mixture, and 5 mM EDTA.

For the cholesterol depletion experiments, the cells were incubated in the presence of 10 μM mevastatin or 0.5 μg/ml filipin for 8 h or with 20 mM methyl β-cyclodextrin (Sigma) for 1 h at 37 °C. For the cholesterol repletion experiments, the cells were incubated in the presence of 10 μM mevastatin and 50 μg/ml cholesterol (Sigma) for 8 h at 37 °C.

Immunofluorescence—Cells were washed and incubated for 25 min at 4 °C with chilled phosphate-buffered saline (PBS) containing 10 μg/ml FITC-conjugated CtxB (Sigma). Then, they were rinsed with warm PBS and fixed by immersion in 4% (w/v) paraformaldehyde in 0.1 M phosphate buffer for 20 min followed by rinsing in PBS, 3 × 15 min. The cells were incubated for 1 h at room temperature (20–22 °C) in a solution containing 2% bovine serum albumin (Sigma) and 0.25% Triton X-100. Double immunolabeling was performed by incubating the cells at room temperature for 1 h in the presence of primary antibodies against β-DG (1/25) and laminin (1/1500) or AQP4 (1:200), syntrophin (1:100) and laminin (1/1500), utrophin (1/10) and dystrophin (1/100), flotillin-1 (1/25) and AQP4 (1/100), or β-DG (1/25) and caveolin-1 (1/100). Subsequently, they were rinsed with PBS (3 × 15 min) and incubated with Alexa Fluor 568 goat anti-mouse IgG and Alexa Fluor 647 goat anti-rabbit or Alexa Fluor 568 goat anti-mouse IgG and Alexa Fluor 488 goat anti-rabbit IgG for 1 h (1/200, Molecular Probes). After several washes with PBS, coverslips were mounted on glass slides using Prolong Gold Antifade reagent with or without 4′,6-diamidino-2-phenylindole (Invitrogen). To confirm the specificity of the labeling, control cells were treated equivalently in the absence of primary antibodies. Fluorescent labeling of cultured cells was visualized using a confocal microscope (Fluoview 1000, Olympus) and an Uplan Apochromat 1.35 numerical aperture 60× objective (Olympus).

Fluorescence Recovery after Photobleaching Analysis—Cortical astrocytes plated in 8-well μ-slides (Ibidi, Munich, Germany) were incubated with 10 μg/ml FITC-CtxB for 20 min. Images were acquired on a confocal microscope (FV1000, Olympus) with an Uplan Apochromat 1.35 numerical aperture 60× objective and fully opened pinhole. Photobleaching of FITC-CtxB was performed for 50 ms using a 405 simultaneous

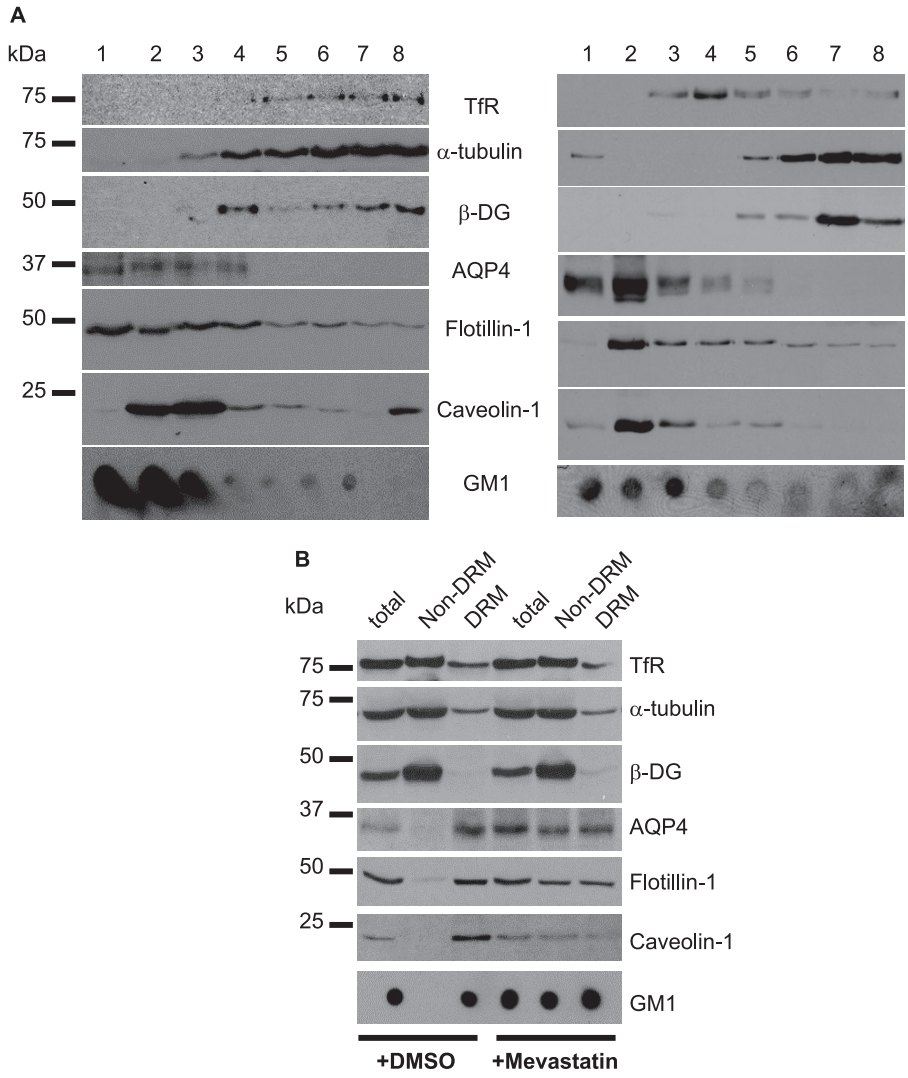

FIGURE 1. **The association of AQP4 with the DRMs is dependent on cholesterol in astrocytes.** *A*, rat cortical astrocytes were solubilized either in 1% Triton X-100 (*left panel*) or detergent-free buffer (*right panel*) and fractionated through a discontinuous sucrose gradient. *B*, astrocytes were incubated with 10 μM mevastatin for 8 h, and proteins were harvested in DRMs and non-DRMs. Immunoblots were probed for the TfR, α-tubulin, β-DG, AQP4, flotillin-1, and caveolin-1, and the dot blot was labeled for GM1. Representative blots from three independent experiments are shown.

scanner set at 60% power within a circular area of 15-pixel diameter. Fluorescence recovery data were collected every second for over 120 s from 8 cells per experiment and analyzed with Prism software (GraphPad) using non-linear regression.

Subcellular Fractionation of Proteins from Astrocyte Cultures—To separate detergent-soluble from -insoluble fractions, the cultured astrocytes were harvested and suspended in 0.5 ml of ice-cold TNE buffer (25 mM Tris-HCl, pH 7.5, 150 mM NaCl, 5 mM EDTA) supplemented with 0.5% Triton X-100 and 1× Complete protease inhibitor mixture. After 20-min incubation on ice, the lysates were centrifuged at 800 × *g* for 10 min. The supernatant was further centrifuged at 100,000 × *g* for 1 h at 4 °C to obtain detergent-resistant membranes (DRMs) and non-detergent-resistant membranes (non-DRMs).

For the flotation assay, astrocyte cultures were harvested and lysed on ice for 30 min in TNE buffer supplemented with 1% Triton X-100 and 1× Complete protease inhibitor mixture. Nuclei and cellular debris were removed from the suspension by centrifugation at 1000 × *g* for 10 min. Other astrocyte cultures were harvested and lysed in a detergent-free buffer using 500 mM sodium carbonate, pH 11.0, as previously described (26). The protein extracts were collected and subjected to a flotation assay using a discontinuous sucrose gradient. To prepare the latter, 1 ml of supernatant was mixed with 3 ml of 85% sucrose in TNE and transferred to the bottom of a Beckman centrifuge tube. The diluted cell lysate was overlaid with 2 ml of 50% sucrose, 3 ml of 35% sucrose, 1 ml of 15% sucrose and finally with 200 μl of TNE buffer. The samples were centrifuged in an SW41 rotor at 200,000 × *g* for 20 h at 4 °C. Fractions numbered 1–8 were collected from the top of the gradient and analyzed by Western and dot blots.

Immunoblotting and Dot Blotting—The samples obtained from siRNA-transfected astrocytes as well as from the subcellular fractionation of astrocyte cultures were denatured by boiling for 9 min in reducing sample buffer and then loaded on a 10% SDS-PAGE gels. The gels were electrotransferred onto nitrocellulose membranes (Bio-Rad, Mississauga, Ontario, Canada), and the blots were probed with antibodies to AQP4 (1/1000), caveolin-1 (1/500), flotillin-1 (1/500), β-DG (1/300), α-tubulin (1/1000), and TfR (1/1000). Bound antibodies were detected using horseradish peroxidase-conjugated goat anti-rabbit IgG or goat anti-mouse IgG (1/2000, Jackson ImmunoResearch). To detect the GM1 ganglioside, 1 μl of each fraction was dotted onto a nitrocellulose membrane and probed with horseradish peroxidase-coupled CtxB (10 ng/ml horseradish peroxidase-CtxB, Sigma). Signals were visualized on Bioflex econo films (Interscience, Markham, Ontario, Canada) using chemiluminescence (Amersham Biosciences).

Quantitative Analyses—The number of clusters, surface area of the clusters, and the colocalization between clusters containing GM1 and β-DG, β-DG and laminin, β-DG and AQP4, laminin and GM1, as well as AQP4 and GM1 were determined on images subjected to a threshold using ImagePro Plus software (Media Cybernetics, Inc.). Signals were considered as clusters when their intensity was above background and above surrounding diffuse immunofluorescence and when their size was at least 1.5 μm^2. Clusters were counted in an average of 15 random fields per treatment, and experiments were repeated at

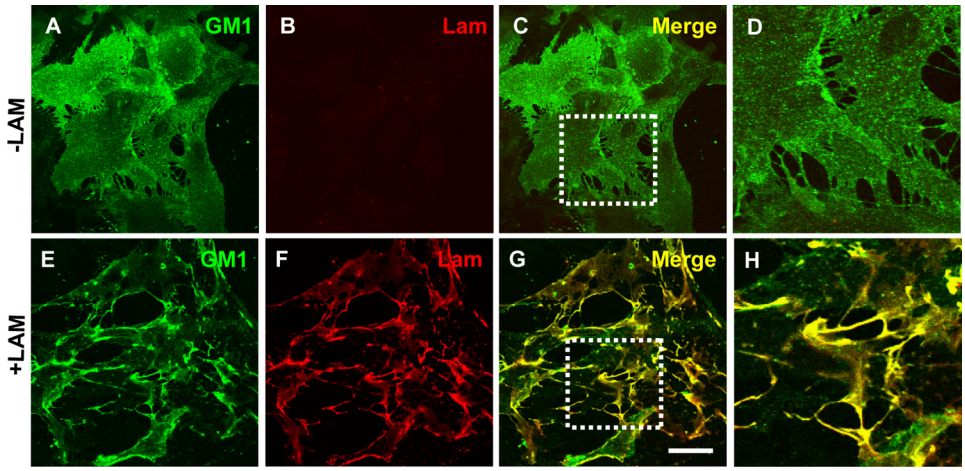

FIGURE 2. **Laminin organizes GM1-containing lipid rafts into clusters in astrocytes.** *A–D*, rat cortical astrocytes incubated in the absence or the presence (*E–H*) of 30 nM laminin were labeled for GM1 using FITC-CtxB (*A* and *E*) and for laminin (*B* and *F*). High magnifications of the *areas boxed* in *C* and *G* are shown in *D* and *H*, respectively. *Scale bar*, 45 μm.

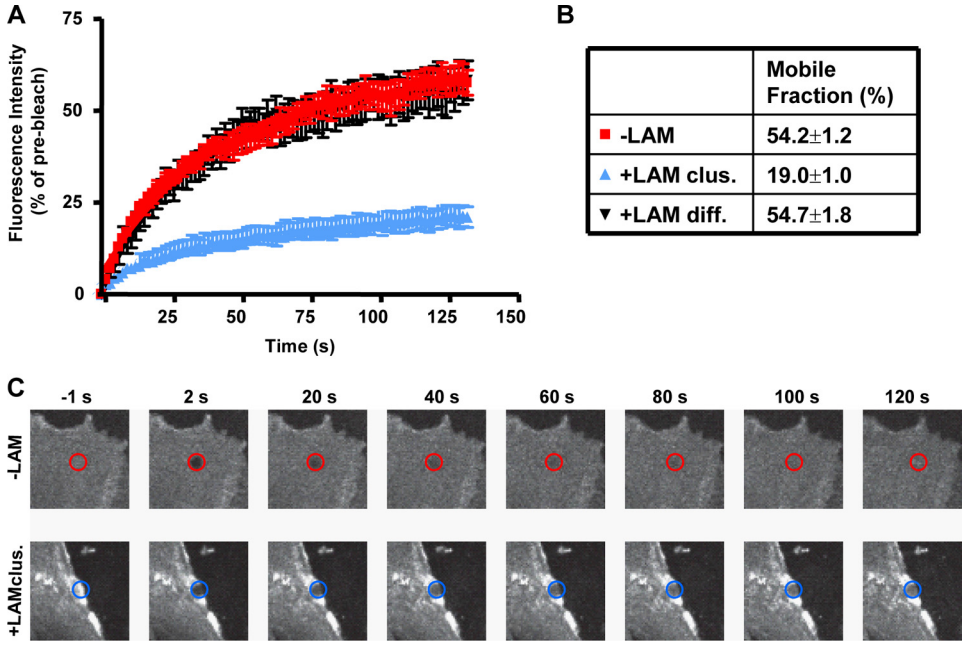

FIGURE 3. **Laminin regulates the membrane diffusion of GM1-containing lipid rafts labeled with FITC-CtxB.** *A*, rat cortical astrocytes treated with 30 nM laminin were incubated with 10 μg/ml FITC-CtxB at room temperature, and areas within CtxB clusters were bleached and imaged for fluorescence recovery. Areas with diffuse FITC-CtxB labeling in both astrocytes treated with laminin and untreated astrocytes were also bleached and imaged for over 120 s. Percent fluorescence intensity ± S.E. in the bleached area during recovery is shown for one representative experiment out of three ($n = 8$ cells/experiment). *B*, percent mobile fraction of FITC-CtxB in areas of untreated astrocytes (−*LAM*), diffuse areas (+*LAM diff.*), and clustered areas of laminin-treated astrocytes (+*LAM clus.*). *C*, representative images of FITC-CtxB-labeled astrocytes are shown before bleaching (−1 s), shortly after bleaching (2 s), and at various time points during fluorescence recovery.

least three times. Images from the same experiment were captured using identical acquisition parameters and subjected to the same threshold. Statistical analyses were performed using GraphPad Prism 3.00 software and unpaired Student's *t* test.

RESULTS

Cholesterol Regulates AQP4 Distribution to Detergent-resistant Membrane Domains in Astrocytes—To determine the distribution pattern of β-DG and AQP4 in lipid raft-containing fractions, Triton X-100 extracts from primary astrocyte cultures were subjected to a flotation assay. The distribution of these proteins was also evaluated in lipid raft fractions obtained using detergent-free astrocytes extracts. The efficiency of the subcellular fractionation was confirmed by probing the obtained fractions with antibodies to the TfR, α-tubulin, flotillin-1, caveolin-1, as well as with horseradish peroxidase-CtxB to detect GM1 (Fig. 1*A*). Fractions 1–4 obtained from Triton X-100 and detergent-free extracts were both enriched for the lipid raft markers flotillin-1, caveolin-1, and GM1 (Fig. 1*A*). As previously described (27), AQP4 was enriched in low density lipid raft-containing fractions 1 to 4 and was not detected in non-lipid raft fractions 5–8 (Fig. 1*A*). However, β-DG co-distributed with the TfR and α-tubulin to fractions 5–8 (Fig. 1*A*). This is in agreement with previous findings showing that β-DG was not found in the GM1-containing lipid raft fractions isolated from embryonic stem cell cultures (28).

We then determined whether the disruption of lipid rafts using mevastatin, filipin, or methyl β-cyclodextrin to deplete membrane cholesterol resulted in alteration of AQP4 distribution in astrocyte cultures. In control astrocytes, we found that the DRM fraction was enriched for flotillin-1 and caveolin-1 as well as GM1 and contained AQP4 but virtually no β-DG (+*DMSO*, Fig. 1*B*). However, high amounts of β-DG were found in the non-DRM fraction (+*DMSO*, Fig. 1*B*), confirming the results obtained using the flotation assay (Fig. 1*A*). In astrocyte cultures treated with either mevastatin (+*Mevastatin*, Fig. 1*B*), filipin (supplemental Fig. S1*A*), or methyl β-cyclodextrin (supplemental Fig. S1*B*), a decrease in the amounts of flotillin-1 and caveolin-1 was observed in the DRM compared with control untreated cells (+*DMSO*, Fig. 1*B*). Moreover, a pool of flotillin-1, caveolin-1, and GM1 translocated to non-DRM confirming that mevastatin (Fig. 1*B*), filipin, and methyl β-cyclodextrin (supplemental Fig. S1) efficiently depleted membrane cholesterol. Most interestingly, AQP4 also partially translocated to non-DRM fractions indicative of the cholesterol-dependent association of a pool of AQP4 with DRM (Fig. 1*B* and supplemental Fig. S1).

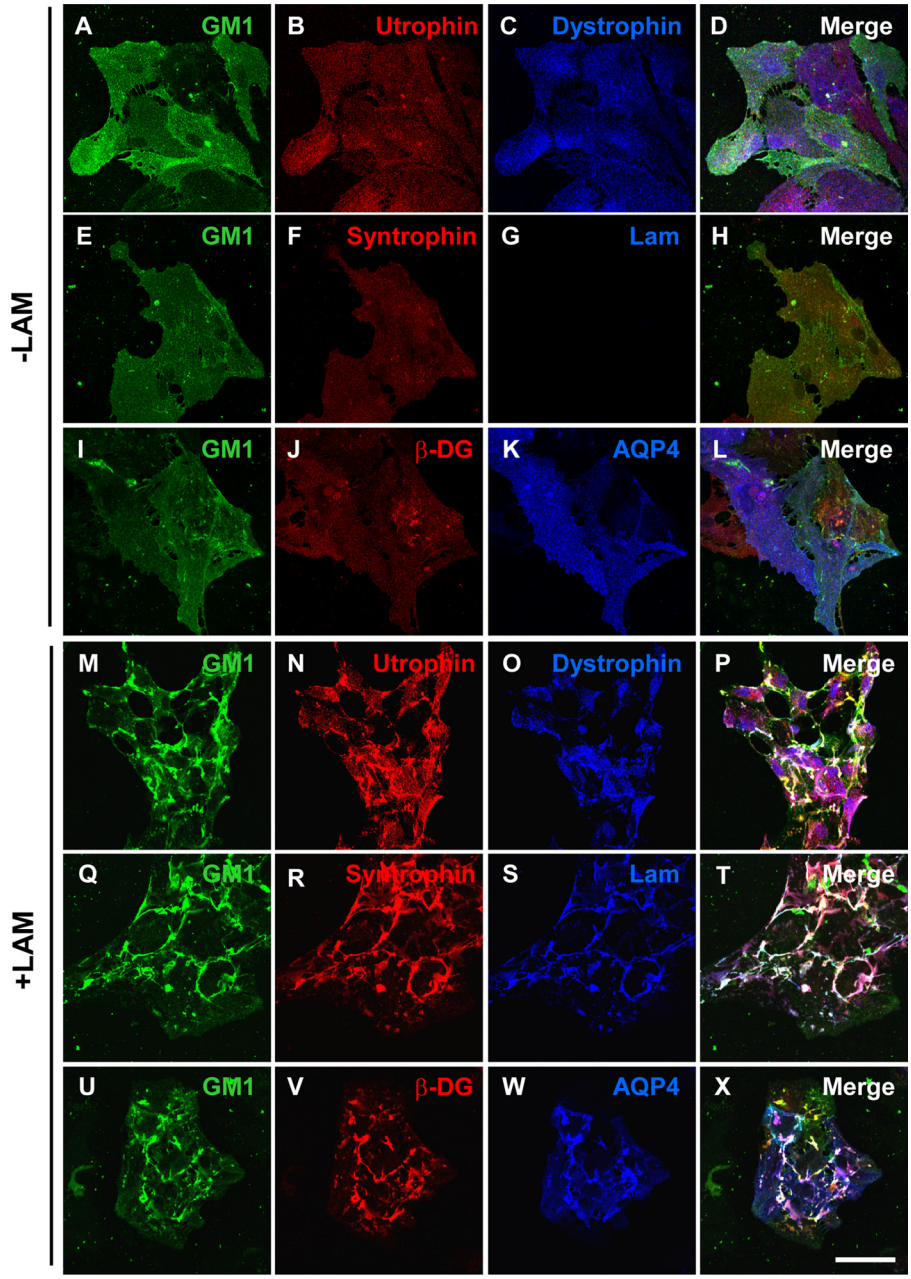

FIGURE 4. **Laminin-induced clustering of the dystrophin complex and AQP4 is associated with the organization of GM1-containing lipid rafts.** *R* rat cortical astrocytes incubated in the absence (*A–L*) or the presence (*M–X*) of 30 nM laminin were first labeled for GM1 using FITC-CtxB and then double immunolabeled for utrophin (*B* and *N*) and dystrophin (*C* and *O*), syntrophin (*F* and *R*) and laminin (*G* and *S*), as well as for β-DG (*J* and *V*) and AQP4 (*K* and *W*). *Scale bar*, 50 μm.

Laminin Induces the Reorganization and Stabilization of GM1 in Astrocytes—To investigate the effect of laminin on the organization of lipid rafts containing the ganglioside GM1, we used FITC-CtxB. In laminin-treated astrocytes, GM1 presented a robust clustering (Fig. 2*E*) compared with control untreated astrocytes where the distribution of GM1 was diffuse (Fig. 2*A*). These clusters presented a high degree of colocalization with the laminin clusters (Fig. 2, *E–H*). Furthermore, laminin did not induce a detectable change in the morphology of astrocytes, because laminin-treated astrocytes presented a flat and polygonal shape similar to that of control untreated astrocytes as assessed by wheat germ agglutinin labeling (supplemental Fig. S2). Together these data show that the laminin-induced reorganization of the raft component GM1 is not associated with a change in astrocyte morphology.

To determine whether laminin-induced clustering of GM1 affected its diffusion in the membrane (29, 30), we performed fluorescence recovery after photobleaching of FITC-CtxB in untreated and laminin-treated astrocytes (Fig. 3). Laminin treatment resulted in a dramatic reduction in the rate of FITC-CtxB recovery but only for FITC-CtxB localized within the laminin-induced clusters (Fig. 3, *A–C*). This shows that laminin stabilizes GM1-bound FITC-CtxB within the clusters and reduces the exchange rate of FITC-CtxB within the bleached region with FITC-CtxB outside the bleached region. Therefore, the colocalization of CtxB and laminin clusters not only reflects a laminin-induced redistribution of GM1 but also reveals a role for laminin in the stabilization of this raft component in astrocyte membrane domains.

Laminin Induces the Coclustering of the DAP Complex, AQP4, and GM1—Given that laminin induces the coclustering of the DAP complex with both Kir4.1 and AQP4 (8), we asked whether this coincided with the laminin-induced clustering of GM1. In the absence of laminin, GM1 labeled with FITC-CtxB was homogeneously distributed throughout the cell (Fig. 4, *A*, *E*, and *I*). Utrophin (Fig. 4*B*), dystrophin (Fig. 4*C*), syntrophin (Fig. 4*F*), β-DG (Fig. 4*J*), and AQP4 (Fig. 4*K*) also exhibited a homogeneous distribution. Upon laminin treatment, CtxB-labeled GM1 coclustered with utrophin and dystrophin (Fig. 4, *M–P*), syntrophin, and laminin (Fig. 4, *Q–T*) as well as with β-DG and AQP4 clusters (Fig. 4, *U–X*). This laminin-induced clustering of these DAP complex components was not accompanied by a change in their expression levels as determined by Western blot analysis (data not shown).

Quantitative analysis revealed over 2-fold increase in the number of GM1 clusters in the laminin-treated compared with the untreated astrocytes that parallels the increase in the number of β-DG, laminin, and AQP4 clusters, as previously reported (Fig. 5*A*) (8, 25). The surface area of GM1-containing

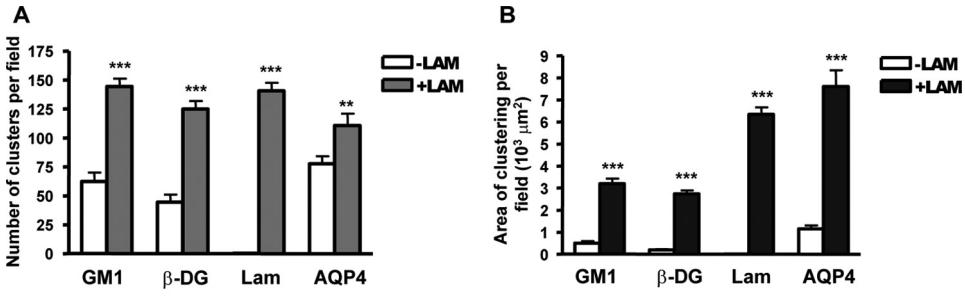

C

	GM1 /β-DG	β-DG /Lam	β-DG / AQP4	Lam /GM1	AQP4 / GM1
+LAM	0.74 ± 0.010***	0.83 ± 0.008***	0.62 ± 0.013***	0.80 ± 0.012***	0.53 ± 0.015***

FIGURE 5. **Quantitative analysis of the laminin-induced clustering of GM1-containing lipid rafts, β-DG, laminin, and AQP4.** *A* and *B*, the histograms represent the mean number of clusters ± S.E. and surface area of clusters ± S.E. in astrocyte cultures treated with laminin (+*LAM*) and control untreated cultures (−*LAM*) from three experiments. The *asterisks* represent statistically significant differences from control (−*LAM*) as assessed by Student's *t* test (***, $p < 0.0001$; **, $p < 0.001$). *C*, the table represents the mean Pearson's colocalization coefficient ± S.E. from three experiments. The *asterisks* represent statistically significant differences from control untreated cells as assessed by Student's *t* test (***, $p < 0.0001$). All quantifications were performed on 15 fields acquired randomly from each experiment.

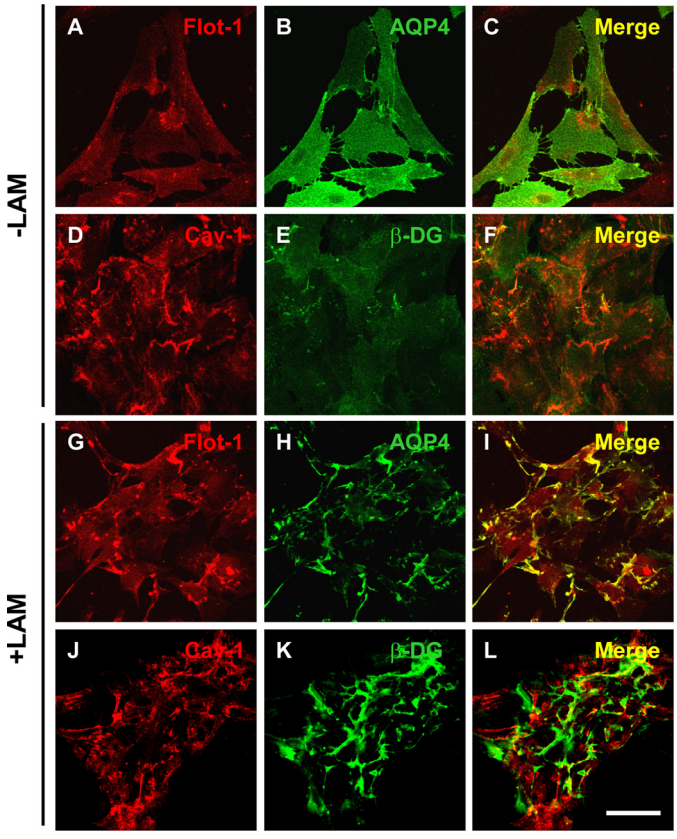

FIGURE 6. **Laminin induces the coclustering of the lipid raft marker flotillin-1 with AQP4 but not of caveolin-1 with β-DG.** Astrocytes incubated in the absence (*A–F*) or the presence (*G–L*) of 30 nM laminin were double immunolabeled for flotillin-1 (*A* and *G*) and AQP4 (*B* and *H*) or caveolin-1 (*D* and *J*) and β-DG (*E* and *K*). *Scale bar*, 50 μm.

clusters increased significantly by >6-fold in the laminin-treated compared with untreated astrocytes, as did the surface area of β-DG and AQP4 (Fig. 5*B*). The higher laminin concentration used in the present study (30 nM instead of 15 nM) may account for the increase in the surface area of these AQP4 clusters relative to a previous study (8). A significant degree of colocalization was found between β-DG, GM1, and AQP4 upon laminin treatment (Fig. 5*C*). These results demonstrate an important role for the ECM and more specifically for laminin in the coclustering of the DAP complex and GM1-containing lipid rafts in astrocytes. In addition, the fluorescence data in Fig. 6 show that flotillin-1, another marker of lipid rafts, underwent clustering upon laminin treatment (Fig. 6*G* compared with Fig. 6*A*) and that these clusters colocalized extensively with AQP4 clusters (Fig. 6, *G–I*). In contrast, the distribution of the lipid raft marker, caveolin-1, did not change upon laminin treatment (Fig. 6, compare *J* to *D*) and remained distinct from β-DG clusters (Fig. 6, *J–L*).

We also observed that laminin induces the coclustering of GM1-containing lipid rafts with β-DG and AChR in C2C12 myotubes (supplemental Fig. S3) as has been previously described for the ECM protein agrin (21, 24, 31, 32). However, this is not the case for GM1 in astrocytes treated with either soluble recombinant C-agrin 4,8 (supplemental Fig. S4*E*) or C-agrin 0,0 (data not shown). Similarly, fibronectin did not induce GM1 clustering (supplemental Fig. S4*I*). These data argue that, in the astrocytes examined in the present study, laminin plays a primary role in GM1 reorganization.

Cholesterol Is Required for the Laminin-induced Coclustering of β-DG, AQP4, and GM1-containing Lipid Rafts—Based on the laminin-induced colocalization of GM1-containing lipid raft clusters with the DAP complex and AQP4 clusters (Figs. 4, *M–X*, and 5*C*), we examined qualitatively and quantitatively whether lipid raft integrity is crucial for the DAP/AQP4 clustering. To disrupt lipid rafts, we used the cholesterol-depleting and -sequestering agents mevastatin and filipin, respectively. Astrocytes treated both with laminin and mevastatin (Fig. 7, *I–P*) or laminin and filipin (supplemental Fig. S5, *G–L*) were fluorescently labeled for GM1, β-DG, laminin, and AQP4. We found that GM1 (Fig. 7, compare *I* and *M* to *A* and *E*), β-DG (Fig. 7, compare *J* and *N* to *B* and *F*), and AQP4 (Fig. 7, compare *O* to *G*) had a uniform distribution and virtually no clustering throughout the cells similar to untreated astrocytes (Fig. 4, *I–L*). Likewise, laminin did not cluster (Fig. 7, compare *K* to *C*) and presented a diffuse immunolabeling pattern. The diffuse immunolabeling is indicative of binding of exogenous laminin that is, however, ineffective in terms of assembling at the cell surface and clustering the DAP complex and AQP4. When astrocytes were incubated in the presence of laminin, mevastatin, and cholesterol, clustering of GM1, β-DG, laminin, and AQP4 was significantly rescued (Fig. 7, *Q–Z*). These data

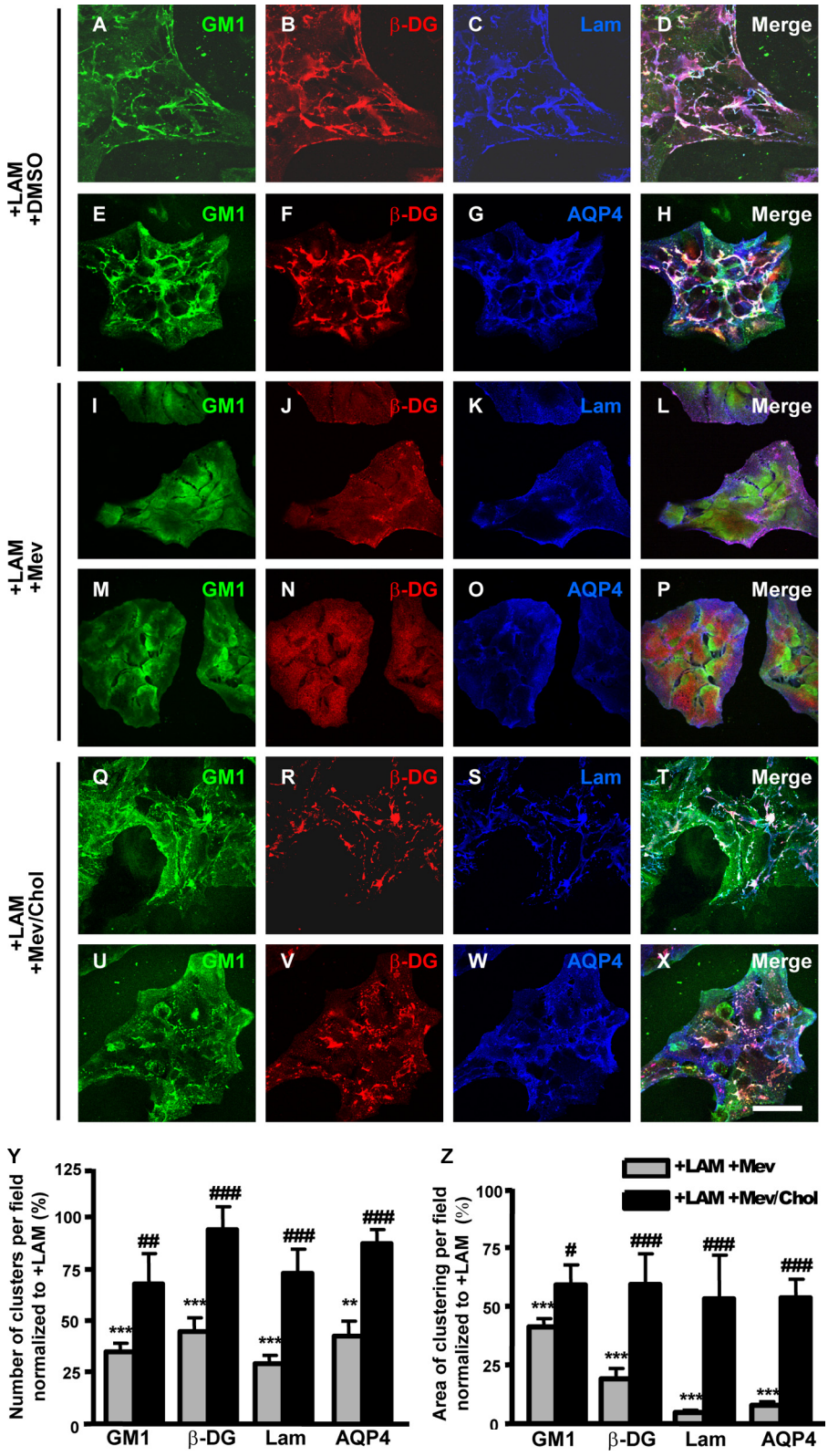

FIGURE 7. **The laminin-induced clustering of GM1, β-DG, and AQP4 is dependent on cholesterol.** *A–H*, Astrocytes incubated in the presence of 30 nM laminin and DMSO (*A–H*), 30 nM laminin and 10 μM mevastatin diluted in DMSO (*I–P*), or 30 nM laminin, 10 μM mevastatin, and 50 μg/ml cholesterol (*Q–X*) were labeled for GM1 (*A*, *I*, and *Q*), β-DG (*B*, *J*, and *R*), and laminin (*C*, *K*, and *S*) or GM1 (*E*, *M*, and *U*), β-DG (*F*, *N*, and *V*), and AQP4 (*G*, *O*, and *W*). *Scale bar*, 50 μm. *Y* and *Z*, the *histograms* represent the mean number of clusters as well as their mean surface area ± S.E. from three different experiments. The quantifications were performed on 15 fields acquired randomly from each experiment. The *asterisks* and *number signs* represent statistically significant differences from laminin and laminin plus mevastatin-treated astrocytes, respectively, as assessed by Student's *t* test (***, $p < 0.0001$; **, $p < 0.001$; #, $p < 0.03$; ##, $p < 0.005$; ###, $p \leq 0.0001$).

show that the laminin-induced cluster formation requires membrane cholesterol.

To assess the effect of cholesterol depletion on the expression levels of α-DG, β-DG, and AQP4, we compared by Western blot the amounts of these proteins in mevastatin-treated astrocytes *versus* untreated astrocytes (supplemental Fig. S6). We found that the expression levels of these proteins are similar in treated and untreated astrocytes, indicating that the decrease in the clustering of DG and AQP4 in mevastatin-treated astrocytes is not a consequence of a reduction in their expression levels. These data demonstrate the cholesterol dependence of laminin-induced cell surface organization and DG and AQP4 clustering.

Dystroglycan Is Required for the Laminin-induced Clustering of GM1—We have previously shown both in astrocytes and Müller glia that the laminin binding receptor α-DG, but not β1-integrin, clusters extensively upon laminin treatment (8, 25). We therefore asked whether DG had a role in the laminin-mediated clustering of GM1. To address this question, we used siRNA to silence DG expression (si*Dag1*) and determined whether this altered the laminin-mediated clustering of GM1 by quantitative fluorescence analysis. As previous evidence demonstrated a dramatic alteration of the morphology of si*Aqp4*-transfected rat astrocytes that occurs between 2 and 6 days after transfection, we carried out our analysis at 2 days following transfection (33, 34). First, we assessed by Western blot the efficiency of the si*Dag1* transfection and found that β-DG could not be detected in the si*Dag1*-transfected cells when compared with the control scrambled siRNA-transfected astrocytes (*siCTL*, Fig. 8*A*) and untransfected astrocytes (data not shown). As an additional control, we used siRNA to silence AQP4 expression (si*Aqp4*) and found that, although this inhibited AQP4 expression, it had no impact on β-DG expression (Fig. 8*A*). Second,

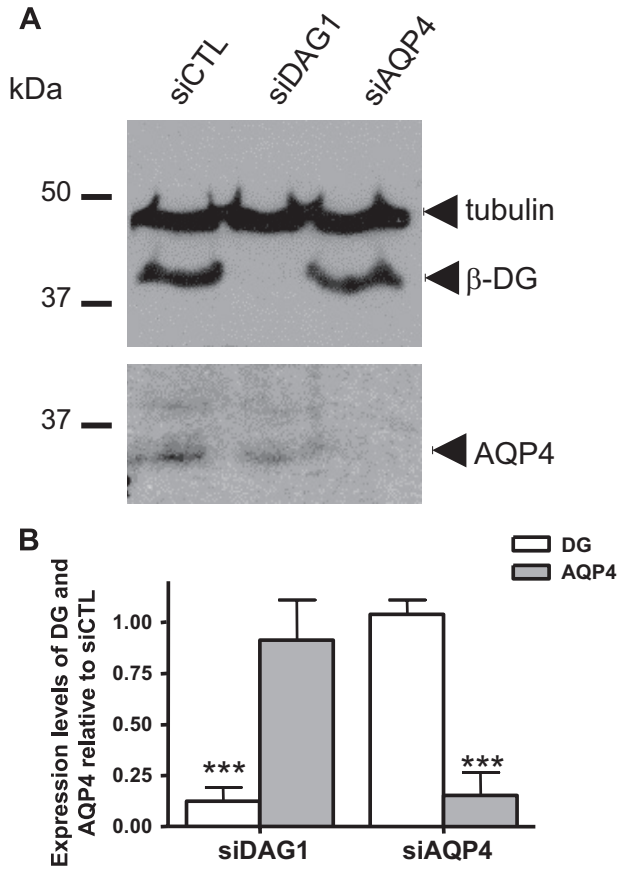

FIGURE 8. **Dystroglycan and AQP4 siRNAs mediate gene silencing in astrocytes.** *A*, Western blot analysis of β-DG and AQP4 was performed 2 days following the transfection of astrocytes with si*Dag1*, si*Aqp4*, and siCTL (scrambled siRNA). *B*, the *histograms* represent the mean expression levels of β-DG and AQP4 ± S.E. from three experiments normalized to tubulin and compared with siCTL. The *asterisks* represent statistically significant differences from control as assessed by Student's *t* test (***, $p < 0.0001$).

we verified that the morphology and the GFAP immunolabeling of the si*Dag1*- and si*Aqp4*-transfected astrocytes were comparable to those of siCTL-transfected cells (supplemental Fig. S7). The data obtained here show a high efficiency of si*Dag1* gene silencing and no detectable effect of either si*Dag1* or si*Aqp4* on astrocyte morphology when compared with siCTL-transfected (supplemental Fig. S7) or to untransfected astrocytes at 2 days post-transfection (data not shown).

The immunofluorescence analysis corroborates the Western blot data (Fig. 8) and shows virtually no immunolabeling for β-DG in the si*Dag1*-transfected astrocytes (Fig. 9, *J* and *N*). However, some small clusters of laminin (Fig. 9*O*) were detected even in the absence of any signal for β-DG (Fig. 9*N*). Of particular interest, the laminin-induced GM1 clustering in the siCTL-transfected astrocytes (Fig. 9, *A* and *E*) was significantly reduced in the si*Dag1*-transfected astrocytes (Fig. 9, *I* and *M*). In addition, the astrocytes deficient for DG exhibited reduced clustering of AQP4 compared with the siCTL astrocytes (Fig. 9, compare *K* to *C*). The si*Aqp4*-transfected astrocytes presented a decrease in AQP4 immunolabeling (Fig. 9, compare *S* to C) and no change in β-DG (Fig. 9, *R* and *V*) and laminin immunolabeling and clustering (Fig. 9*W*) compared with control cells (Fig. 9, *B*, *F*, and *G*). In addition, the laminin-induced clustering of GM1 was not affected by AQP4 silencing (Fig. 9, *Q* and *U*). It is noteworthy that the effect of si*Dag1* was more pronounced on the surface area of the GM1, β-DG, laminin, and AQP4 clusters than on their number (Fig. 10, compare *B* to *A*). This suggests that, despite the fact that a small proportion of these clusters can form, their size is dramatically reduced in astrocytes deficient for DG.

DISCUSSION

Laminin Coclusters GM1 with the DAP Complex and AQP4 in Astrocytes—In brain, astrocytes are polarized and present an asymmetrical distribution of proteins such as DG and AQP4 that are diffusely distributed along the astrocyte processes in the parenchyma but highly concentrated at astrocyte endfeet abutting blood vessels. Astrocyte endfeet interact with the perivascular ECM, and previous studies have shown both *in vivo* and *in vitro* that astrocyte interaction with laminin via DG is essential for the concentration of several members of the DAP complex as well as Kir4.1 and AQP4 at specialized astrocyte membrane domains (6, 8, 12). Although such a distribution is functionally important in potassium ion and water homeostasis, the mechanisms regulating the formation of these Kir4.1- and AQP4-enriched domains remain to be elucidated. AQP4 is associated with lipid raft-containing fractions in both brain and retina (27, 35) as is another aquaporin, AQP5, that participates in fluid secretion in parotid gland cells (36). We therefore undertook a study to evaluate the role of lipid rafts in laminin-DG-dependent AQP4 clustering, and our data show that laminin induced a dramatic redistribution of GM1 into large cell surface clusters or macrodomains that colocalized extensively with β-DG and AQP4. The recruitment of AQP4 to laminin-rich clusters is therefore interdependent on both DG and cholesterol-rich lipid raft domains.

The DAP complex and AQP4 associate in a subset of rafts containing GM1 and flotillin-1 distinct from caveolin-1-containing caveolae. Indeed, flotillin has been reported to be localized to lipid raft domains distinct from caveolin-1 (37). Laminin therefore promotes coclustering of the DAP complex and AQP4 with a select population of lipid rafts in astrocyte membrane domains. How these coclusters of the DAP complex and AQP4/GM1/flotillin-containing lipid rafts are organized remains uncertain. In fact, laminin-induced clustering does not result in the recruitment of β-DG to DRMs (supplemental Fig. S8). Raft-dependent laminin remodeling may induce spatial reorganization in the membrane such that the DAP complex and lipid rafts coexist and interact within the same polarized macrodomain. Indeed, the fact that GM1-bound CtxB exhibits reduced exchange in laminin-induced clusters shows that lipid raft dynamics and behavior are altered within these large membrane domains.

Laminin-induced Coclustering of GM1, the DAP Complex, and AQP4 Depends on the Integrity of Lipid Rafts and Dystroglycan—Cholesterol depletion experiments show that the integrity of lipid rafts is essential not only for the recruitment of AQP4 to DRMs (27) but also for the laminin-dependent assembly of the AQP4, β-DG, and GM1-enriched domains. Conversely, DG silencing resulted in the disruption of laminin assembly and a significant decrease of clustering of not only AQP4 and β-DG at the cell surface but also the raft marker

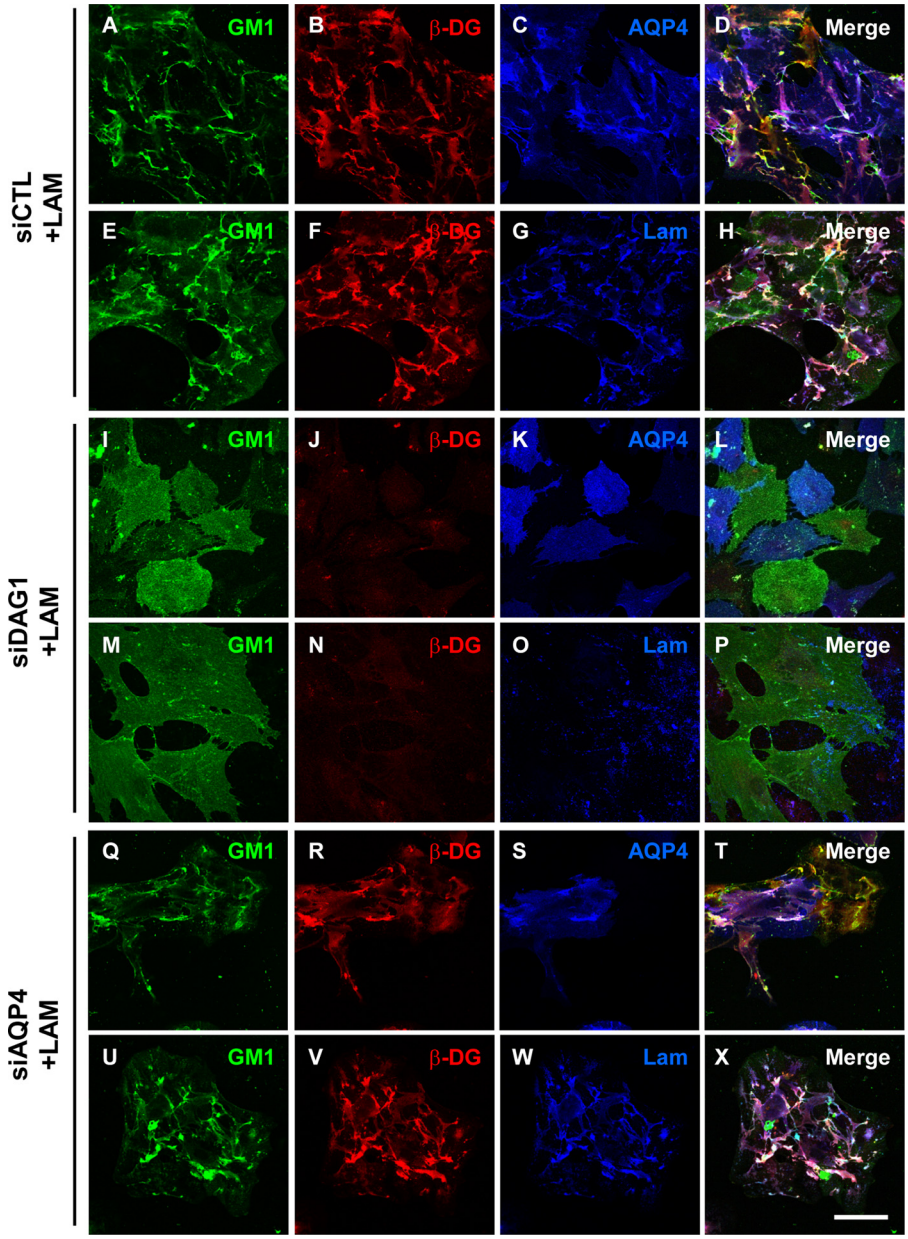

FIGURE 9. **Dystroglycan is essential for the laminin-induced GM1-containing lipid raft, β-DG, and AQP4 coclustering.** Astrocytes were transfected with siCTL (*A–H*), si*Dag1* (*I–P*), or si*Aqp4* (*Q–X*) and incubated with 30 nM laminin. They were then incubated with FITC-CtxB to label GM1 (*A*, *E*, *I*, *M*, *Q*, and *U*) and double immunolabeled for β-DG (*B*, *J*, and *R*) and AQP4 (*C*, *K*, and *S*) or β-DG (*F*, *N*, and *V*) and laminin (*G*, *O*, and *W*). *Scale bar*, 50 μm.

GM1. Coordinate plasma membrane domain organization by both lipid rafts and laminin binding to the DG complex may therefore restrict lateral diffusion of AQP4 within the plasma membrane shedding new light on the mechanisms involved in the polarized distribution of AQP4, and the DAP complex, at perivascular astrocyte endfeet.

Interestingly, the coclustering of GM1 and β-DG with AQP4 and AChRs in astrocytes and C2C12 myotubes (supplemental Fig. S3), respectively, is consistent with a role for laminin in orchestrating the distribution of both lipids and a specific set of proteins to establish functional membrane domains. In C2C12 myotubes, laminin-induced coclustering of components of the DAP complex with AChRs requires Src- and Fyn-dependent tyrosine phosphorylation that enhances the association of postsynaptic proteins with cholesterol-rich membrane domains leading to the stabilization of AChR-containing synapses in muscle (32). Laminin-mediated clustering of α6β1-integrin within the platelet-derived growth factor receptor-containing lipid rafts in oligodendrocytes creates a signaling environment that promotes survival of these cells (22). Furthermore, integrin-mediated adhesion to the ECM regulates Rac1 signaling by preventing internalization of lipid raft-containing membrane domains (38). More recently, the laminin-mediated clustering of GM1 and the agrin association with lipid rafts have both been involved in promoting neurite outgrowth by activating Lyn/Akt/MAPK and Fyn/MAPK signaling pathways, respectively (39, 40). These data define a role for the ECM in regulating raft-associated signaling. It is therefore likely that the laminin-mediated reorganization of GM1-containing lipid rafts and coclustering with the DAP complex provides a signaling environment that promotes the formation of AQP4-rich membrane domains in astrocytes.

Potential Role of Laminin and Lipid Raft-dependent Clustering of AQP4 on Its Activity—AQP4 is the main structural component of intramembrane particles called orthogonal arrays of particles (41–43). Recently, an increase of the density of orthogonal arrays of particles as well as an increase in AQP4 expression accompanied by a more efficient water transport have been reported in astrocytes treated with the ECM molecule, agrin (44). This substantiates further the role of the ECM in the formation of assemblies of orthogonal arrays of particles rich in AQP4 at astrocyte endfeet. Mislocalization of AQP4 at perivascular astrocyte endfeet in the Large^{myd} mouse (6, 12) and loss of its clustering in astrocytes deficient in DG may cause the dispersion or a decrease in the density of orthogonal arrays of particles at these specialized domains that will ultimately alter water transport.

Recent studies have reported that lack of the lipid raft gangliosides GM1 and GD1 (45) or depletion of cholesterol resulted in abnormal paranodal sodium channel clusters in the peripheral nervous system and prevented the agrin-induced

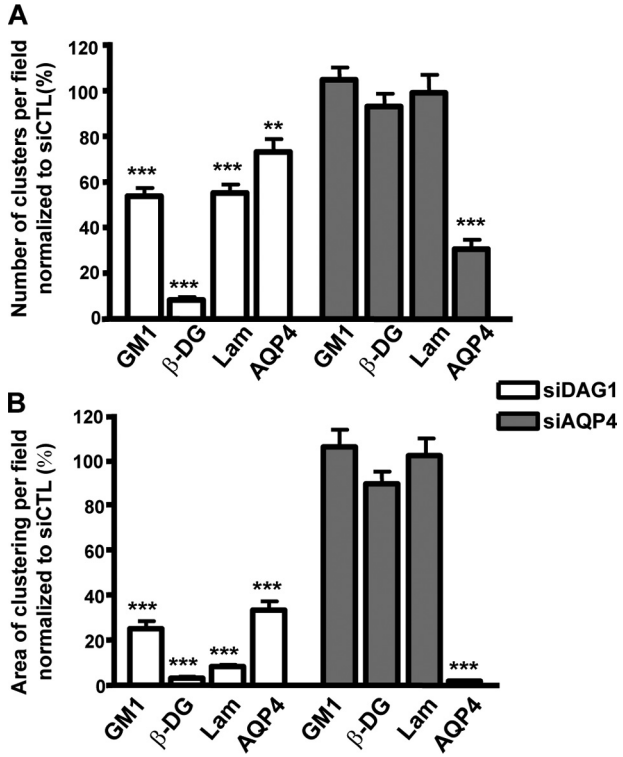

FIGURE 10. **Quantitative analysis of the effect of the dystroglycan silencing on the laminin-induced clustering of GM1-containing lipid rafts, β-DG, and AQP4.** *A* and *B*, the *histograms* represent the mean number of clusters ± S.E. and surface area of clusters ± S.E. in astrocyte cultures from three experiments. The *asterisks* represent statistically significant differences from control siCTL-transfected cells as assessed by Student's *t* test (***, $p < 0.0001$). All quantifications were performed on 15 fields acquired randomly from each experiment.

clustering of AChRs in C2C12 myotubes, respectively (31, 45, 46). Moreover, cholesterol depletion in neuronal cultures decreases the number of synapses and α-amino-3-hydroxy-5-methyl-4-isoxazolpropionic acid receptor stability (47). In some instances, it has been demonstrated that cholesterol can influence the activity of ion channels (19, 48). These data raise the interesting hypothesis that lipid rafts may participate in the regulation of the AQP4 channel properties that define its role in water transport.

The present study demonstrates that loss of interaction between laminin and DG mimics the effect of membrane cholesterol depletion on AQP4 clustering and points to a concerted action between lipid rafts and ligand binding to DG that leads to the formation of membrane specializations at specific astrocytic sites. These findings therefore implicate lipid rafts in the polarization of the DAP complex and AQP4 in astrocyte endfeet and potentially in AQP4-mediated water transport.

Acknowledgment—We thank Dr. M. Ferns for providing recombinant C-agrin 4,8 and C-agrin 0,0.

REFERENCES

1. Arikawa-Hirasawa, E., Rossi, S. G., Rotundo, R. L., and Yamada, Y. (2002) *Nat. Neurosci.* **5,** 119–123
2. Marangi, P. A., Wieland, S. T., and Fuhrer, C. (2002) *J. Cell Biol.* **157,** 883–895
3. Nishimune, H., Valdez, G., Jarad, G., Moulson, C. L., Müller, U., Miner, J. H., and Sanes, J. R. (2008) *J. Cell Biol.* **182,** 1201–1215
4. Ruegg, M. A., and Bixby, J. L. (1998) *Trends Neurosci.* **21,** 22–27
5. Huh, K. H., and Fuhrer, C. (2002) *Mol. Neurobiol.* **25,** 79–112
6. Michele, D. E., Barresi, R., Kanagawa, M., Saito, F., Cohn, R. D., Satz, J. S., Dollar, J., Nishino, I., Kelley, R. I., Somer, H., Straub, V., Mathews, K. D., Moore, S. A., and Campbell, K. P. (2002) *Nature* **418,** 417–422
7. Amiry-Moghaddam, M., Otsuka, T., Hurn, P. D., Traystman, R. J., Haug, F. M., Froehner, S. C., Adams, M. E., Neely, J. D., Agre, P., Ottersen, O. P., and Bhardwaj, A. (2003) *Proc. Natl. Acad. Sci. U.S.A.* **100,** 2106–2111
8. Guadagno, E., and Moukhles, H. (2004) *Glia* **47,** 138–149
9. Zaccaria, M. L., Di Tommaso, F., Brancaccio, A., Paggi, P., and Petrucci, T. C. (2001) *Neuroscience* **104,** 311–324
10. Blake, D. J., Hawkes, R., Benson, M. A., and Beesley, P. W. (1999) *J. Cell Biol.* **147,** 645–658
11. Moukhles, H., and Carbonetto, S. (2001) *J. Neurochem.* **78,** 824–834
12. Rurak, J., Noel, G., Lui, L., Joshi, B., and Moukhles, H. (2007) *J. Neurochem.* **103,** 1940–1953
13. Dalloz, C., Sarig, R., Fort, P., Yaffe, D., Bordais, A., Pannicke, T., Grosche, J., Mornet, D., Reichenbach, A., Sahel, J., Nudel, U., and Rendon, A. (2003) *Hum. Mol. Genet.* **12,** 1543–1554
14. Nico, B., Frigeri, A., Nicchia, G. P., Corsi, P., Ribatti, D., Quondamatteo, F., Herken, R., Girolamo, F., Marzullo, A., Svelto, M., and Roncali, L. (2003) *Glia* **42,** 235–251
15. Frigeri, A., Nicchia, G. P., Nico, B., Quondamatteo, F., Herken, R., Roncali, L., and Svelto, M. (2001) *FASEB J.* **15,** 90–98
16. Amiry-Moghaddam, M., Williamson, A., Palomba, M., Eid, T., de Lanerolle, N. C., Nagelhus, E. A., Adams, M. E., Froehner, S. C., Agre, P., and Ottersen, O. P. (2003) *Proc. Natl. Acad. Sci. U.S.A.* **100,** 13615–13620
17. Amiry-Moghaddam, M., Xue, R., Haug, F. M., Neely, J. D., Bhardwaj, A., Agre, P., Adams, M. E., Froehner, S. C., Mori, S., and Ottersen, O. P. (2004) *FASEB J.* **18,** 542–544
18. Vajda, Z., Pedersen, M., Füchtbauer, E. M., Wertz, K., Stødkilde-Jørgensen, H., Sulyok, E., Dóczi, T., Neely, J. D., Agre, P., Frøkiaer, J., and Nielsen, S. (2002) *Proc. Natl. Acad. Sci. U.S.A.* **99,** 13131–13136
19. Barrantes, F. J. (1993) *Braz. J. Med. Biol. Res.* **26,** 553–571
20. Gee, S. H., Montanaro, F., Lindenbaum, M. H., and Carbonetto, S. (1994) *Cell* **77,** 675–686
21. Stetzkowski-Marden, F., Gaus, K., Recouvreur, M., Cartaud, A., and Cartaud, J. (2006) *J. Lipid Res.* **47,** 2121–2133
22. Baron, W., Decker, L., Colognato, H., and ffrench-Constant, C. (2003) *Curr. Biol.* **13,** 151–155
23. Pike, L. J. (2006) *J. Lipid Res.* **47,** 1597–1598
24. Khan, A. A., Bose, C., Yam, L. S., Soloski, M. J., and Rupp, F. (2001) *Science* **292,** 1681–1686
25. Noël, G., Belda, M., Guadagno, E., Micoud, J., Klöcker, N., and Moukhles, H. (2005) *J. Neurochem.* **94,** 691–702
26. Song, K. S., Li, Shengwen, Okamoto, T., Quilliam, L. A., Sargiacomo, M., and Lisanti, M. P. (1996) *J. Biol. Chem.* **271,** 9690–9697
27. Hibino, H., and Kurachi, Y. (2007) *Eur. J. Neurosci.* **26,** 2539–2555
28. Shah, W. A., Peng, H., and Carbonetto, S. (2006) *J. Gen. Virol.* **87,** 673–678
29. Kenworthy, A. K. (2007) *Methods Mol. Biol.* **398,** 179–192
30. Lajoie, P., Partridge, E. A., Guay, G., Goetz, J. G., Pawling, J., Lagana, A., Joshi, B., Dennis, J. W., and Nabi, I. R. (2007) *J. Cell Biol.* **179,** 341–356
31. Stetzkowski-Marden, F., Recouvreur, M., Camus, G., Cartaud, A., Marchand, S., and Cartaud, J. (2006) *J. Mol. Neurosci.* **30,** 37–38
32. Willmann, R., Pun, S., Stallmach, L., Sadasivam, G., Santos, A. F., Caroni, P., and Fuhrer, C. (2006) *EMBO J.* **25,** 4050–4060
33. Nicchia, G. P., Frigeri, A., Liuzzi, G. M., and Svelto, M. (2003) *FASEB J.* **17,** 1508–1510
34. Benfenati, V., Nicchia, G. P., Svelto, M., Rapisarda, C., Frigeri, A., and Ferroni, S. (2007) *J. Neurochem.* **100,** 87–104
35. Fort, P. E., Sene, A., Pannicke, T., Roux, M. J., Forster, V., Mornet, D., Nudel, U., Yaffe, D., Reichenbach, A., Sahel, J. A., and Rendon, A. (2008) *Glia* **56,** 597–610
36. Ishikawa, Y., Cho, G., Yuan, Z., Inoue, N., and Nakae, Y. (2006) *Biochim. Biophys. Acta* **1758,** 1053–1060
37. Glebov, O. O., Bright, N. A., and Nichols, B. J. (2006) *Nat. Cell Biol.* **8,** 46–54

38. del Pozo, M. A., Alderson, N. B., Kiosses, W. B., Chiang, H. H., Anderson, R. G., and Schwartz, M. A. (2004) *Science* **303,** 839–842
39. Ichikawa, N., Iwabuchi, K., Kurihara, H., Ishii, K., Kobayashi, T., Sasaki, T., Hattori, N., Mizuno, Y., Hozumi, K., Yamada, Y., and Arikawa-Hirasawa, E. (2009) *J. Cell Sci.* **122,** 289–299
40. Ramseger, R., White, R., and Kröger, S. (2009) *J. Biol. Chem*. **284,** 7697–7705
41. Sasaki, H., Kishiye, T., Fujioka, A., Shinoda, K., and Nagano, M. (1996) *Cell Struct. Funct.* **21,** 133–141
42. Verbavatz, J. M., Ma, T., Gobin, R., and Verkman, A. S. (1997) *J. Cell Sci.* **110,** 2855–2860
43. Rash, J. E., Davidson, K. G., Yasumura, T., and Furman, C. S. (2004) *Neuroscience* **129,** 915–934
44. Noell, S., Fallier-Becker, P., Beyer, C., Kröger, S., Mack, A. F., and Wolburg, H. (2007) *Eur. J. Neurosci.* **26,** 2109–2118
45. Susuki, K., Baba, H., Tohyama, K., Kanai, K., Kuwabara, S., Hirata, K., Furukawa, K., Furukawa, K., Rasband, M. N., and Yuki, N. (2007) *Glia* **55,** 746–757
46. Campagna, J. A., and Fallon, J. (2006) *Neuroscience* **138,** 123–132
47. Hering, H., Lin, C. C., and Sheng, M. (2003) *J. Neurosci.* **23,** 3262–3271
48. Romanenko, V. G., Rothblat, G. H., and Levitan, I. (2002) *Biophys. J.* **83,** 3211–3222